Systematics of alpha-cluster states above double shell closures

B. Buck
Department of Physics, University of Oxford, Theoretical Physics, 1 Keble Road, Oxford OX1 3NP, United Kingdom

A. C. Merchant and S. M. Perez*
Department of Physics, University of Oxford, Nuclear Physics Laboratory, Keble Road, Oxford OX1 3RH, United Kingdom
(Received 22 August 1994)

Alpha-particle cluster models have been very successful in reproducing energy spectra, static and dynamic electromagnetic properties, α-emission widths and α-nucleus elastic scattering data in light nuclei around the double shell closures at ^{16}O and ^{40}Ca. We extend the application of one such model to the heavier mass regions above ^{90}Zr and ^{208}Pb. In all cases we employ a potential of given geometric form with all parameters fixed except for the radius that is tailored to each nucleus in turn. We find that the potentials needed for ^{20}Ne and ^{44}Ti are very similar to the real parts of the optical potentials used in an accurate description of α-^{16}O and α-^{40}Ca elastic scattering up to high energies. By suitable choice of the quantum numbers that describe the relative motion of the α particle and the core nucleus we are able to give a good account of the spectra, the reduced $E2$ transition strengths, and the α-particle emission widths (or lifetimes) of the members of the ground state bands in the four nuclei ^{20}Ne, ^{44}Ti, ^{94}Mo, and ^{212}Po. The potential chosen also allows a consistent description of the half-lives for favored α-decay throughout the Periodic Table.

PACS number(s): 21.60.Gx, 23.20.Lv, 23.60.+e, 25.55.Ci

I. INTRODUCTION

The existence of α-particle cluster states in light nuclei has been accepted for a long time. Their presence is experimentally indicated by strong selective excitation in α-transfer reactions, rotationally spaced energy levels, enhanced electromagnetic moments and transition strengths, and appreciable α widths for resonant states above threshold. Another key feature of α-particle spectra is that a band of negative parity states is expected to lie a few MeV above the lowest lying positive parity band. These experimental properties have been well reproduced by a variety of cluster models, including some which are based on effective N-N interactions and treat antisymmetry exactly [1,2]. All of the above-mentioned characteristics are most readily seen experimentally and most easily calculated theoretically in the case of an α particle orbiting a doubly magic core, where binding energy considerations make the cluster-core system especially stable and both constituents have spin zero so that no complications arise from noncentral forces. Amongst light nuclei ^{20}Ne provides an essentially perfect illustration of the properties outlined above [3] (see Fig. 1).

The question immediately arises as to whether similar states exist in heavier nuclei. The obvious place to look is around higher mass doubly closed shell nuclei. Indeed, after initial scepticism, there is now good evidence of α-cluster structure around A=40, with ^{44}Ti being a prime example [4]. The ground state band is strongly populated in the (^{6}Li,d) reaction and is known up to its termination at 12^+, the levels are connected by strong $E2$ transitions, and the first few members of the accompanying negative parity band have been located recently [5,6]. These properties are well described by several cluster models [7–9]. In all cases the α-^{40}Ca potential employed is compatible with the real part of the optical potential deduced from elastic α-particle scattering, which has been carefully measured up to energies where the anomalous large angle scattering (ALAS) phenomenon is apparent [10].

Does such cluster structure persist at higher mass numbers? The obvious places to look are above the double shell closures at ^{90}Zr and ^{208}Pb in ^{94}Mo and ^{212}Po, respectively. Such systems are too complicated for a fully microscopic treatment, and we shall have to rely on more phenomenological models to predict cluster state properties and to interpret the available data. We believe that there are already sufficient indications that an α-cluster interpretation is a fruitful way to understand the properties of the ground state bands of these two heavier nuclei.

The existence of α decay in heavy nuclei suggests a non-negligible probability for finding α particles preformed in the parent nucleus. We have previously been able to give a good quantitative description of the half-lives for α decays in a wide range of heavy nuclei using a preformed α-cluster model [11,12]. Unfortunately, this does not enable us to say anything definite about the value of the α particle preformation probability except that it appears to vary remarkably little from one nucleus to another. Recently however, more microscopic calcu-

*Permanent address: Department of Physics, University of Cape Town, Private Bag, Rondebosch 7700, South Africa.

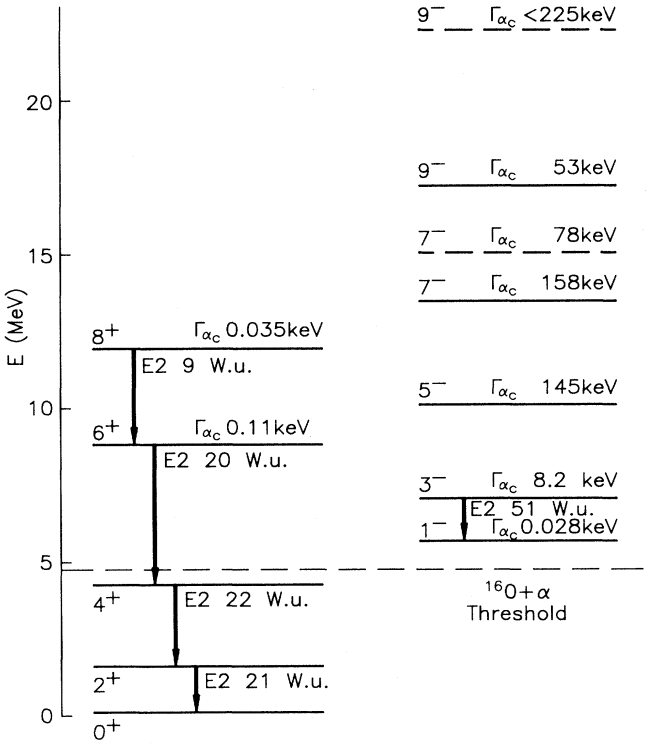

FIG. 1. Positive and negative parity bands of α-cluster states in ^{20}Ne showing quasirotational spectra, enhanced in-band $E2$ transitions, and significant α-emission widths (their principal decay mode).

lations invoking a mixed cluster and shell model basis have suggested a large α particle preformation probability of ~ 0.3 in ^{212}Po [13], and it is not inconceivable that the preformation factor is even larger ($P \sim 1$). If this is so, it suggests that the low lying spectrum of ^{212}Po is explicable in terms of an α-^{208}Pb cluster model. A preliminary investigation has already shown that the $E2$ transition rates and α-decay half-lives of the members of the ground state band can be well described in this way [14]. However, both this calculation and our wider ranging α decay calculations are insensitive [11] to the geometric form of the α-core potential. In order to calculate the energy levels correctly, a more careful description of the interior of the α-nucleus potential is required. We propose to employ the same type of phenomenological α-cluster model which has been successful in describing α decay, but modified so as to describe simultaneously the spectra of ^{20}Ne, ^{44}Ti, ^{94}Mo, and ^{212}Po in a unified way with a fixed set of parameters. At the same time we shall insist on preserving an adequate description of α-decay half lives in heavy nuclei and compatibility with the real parts of the optical potentials determined from α-^{16}O [15] and α-^{40}Ca [10] elastic scattering. The general features of such a unified potential could then be retained in future calculations, with parameters fine-tuned to the application at hand.

II. THE α-CLUSTER MODEL

We employ a variation of the local potential cluster model first introduced by Buck, Dover, and Vary [3]. A preformed, inert α cluster interacts with a core through a local potential $V(r)$ containing nuclear, Coulomb, and centrifugal terms

$$V(r) = -V_0 f(r, R, a, \alpha) + V_C(r) + \frac{\hbar^2 L(L+1)}{2\mu r^2}. \quad (1)$$

The nuclear potential is characterized by a depth V_0, radius R, diffuseness a, and any other parameters α necessary to specify its geometry. The values of V_0, a, and α are fixed for all nuclei, but the radius R is fitted separately for each nucleus. The Coulomb potential is taken to be that of a point α particle interacting with a uniformly charged spherical core:

$$V_C(r) = \frac{Z_1 Z_2 e^2}{r} \quad \text{for } r \geq R_C$$
$$= \frac{Z_1 Z_2 e^2}{2R_C}\left[3 - \left(\frac{r}{R_C}\right)^2\right] \quad \text{for } r \leq R_C. \quad (2)$$

We take $R_C = R$ so that the number of adjustable parameters is reduced to one for each nucleus.

The solutions of the single-particle Schrödinger equation with the potential of Eq. (1) are interpreted as bound and resonant states of the cluster-core system, so that the eigenvalues yield the energy spectrum and the associated wave functions may be used to calculate other observable quantities. The major requirements of the Pauli principle are satisfied by restricting the quantum numbers of relative motion to values compatible with an α cluster consisting of nucleons in shell model orbitals above those already occupied by the core nucleons, though this recipe should be regarded as a fairly reliable guide rather than as giving a completely determined parameter. The number of internal nodes n in the radial wave function and the orbital angular momentum L of the relative motion must satisfy

$$2n + L = G, \quad (3)$$

where $G \geq 8$ for ^{16}O+α, $G \geq 12$ for ^{40}Ca+α, etc. Those states in a given nucleus sharing a common even value of G form a positive parity band with $L = 0(2)G$, terminating at $L = G$. Similarly, negative parity bands are associated with an odd value of G, having $L = 1(2)G$. Thus G is a global quantum number which identifies a band of levels.

The fitting procedure to be described in the next section can be implemented in semiclassical approximation without significant loss of accuracy. Energies of bound and quasibound states are obtained using the Bohr-Sommerfeld quantization rule

$$\int_{r_1}^{r_2} dr \sqrt{\frac{2\mu}{\hbar^2}\,|E(n,L) - V(r)|} = (2n+1)\frac{\pi}{2}$$
$$= (G - L + 1)\frac{\pi}{2}, \quad (4)$$

where r_1 and r_2 are the two innermost classical turning points. The Langer modified form of the centrifugal potential is used, with $L(L+1)$ replaced by $(L+\frac{1}{2})^2$. A semiclassical prescription [16] is then employed to evaluate the small widths for α emission. The details are in our previous work [11,12].

The semiclassical calculations described above (or their fully quantum mechanical counterparts, if wave functions are needed) require specification of the geometric form of the nuclear part of the cluster-core potential $f(r,R,a,\alpha)$. Various forms have been successfully employed to describe the quasirotational energy spectrum of the ground state band in ^{20}Ne, and neighboring nuclei. These include Gaussian, squared Woods-Saxon, and "cosh" potentials. However, none of these is satisfactory when extrapolated to very heavy nuclei with unchanged depth and diffuseness values. Indeed, they can even generate inverted spectra where the 0^+ member of a band has the highest excitation energy and the $G = L$ member the lowest.

The problem of how to generate satisfactory spectra for the yrast bands of ^{20}Ne, ^{44}Ti, ^{94}Mo, and ^{212}Po with a given geometry whose only variable parameter is its radius is quite acute (see Fig. 2). For ^{20}Ne the levels are almost rotationally spaced (although the 8^+ is lower than expected). For ^{44}Ti the low spin states are rotationally spaced, but the higher spin states 8^+, 10^+, and 12^+ are tightly compressed. The ^{94}Mo and ^{212}Po ground state bands deviate strongly from an $L(L+1)$ energy dependence.

After a fair amount of trial and error we have settled on the form

$$f(r,R,a,\alpha) = \left\{ \frac{\alpha}{1+\exp[(r-R)/a]} + \frac{1-\alpha}{\{1+\exp[(r-R)/3a]\}^3} \right\} \quad (5)$$

which (with fixed values of V_0, a, and α) is capable of maintaining a good description of the α-decay half-lives of the many heavy nuclei previously examined [12], while simultaneously accounting for the spectra of our four chosen nuclei, as well as producing potentials for the α-^{16}O [15] and α-^{40}Ca [10] systems which are compatible with the real parts of the optical potentials deduced from an extensive sequence of elastic scattering experiments. Of course, our trials of geometric forms could not be exhaustive, and are not necessarily optimal. Nevertheless, the geometry proposed in Eq. (5) has a particularly simple form and achieves our stated aims with a minimum of freely adjustable parameters. Ideally, one would prefer to extract all potentials by model independent inversion techniques from extensive bound state and scattering information. Although we are pursuing this goal, it is a long term project of uncertain outcome.

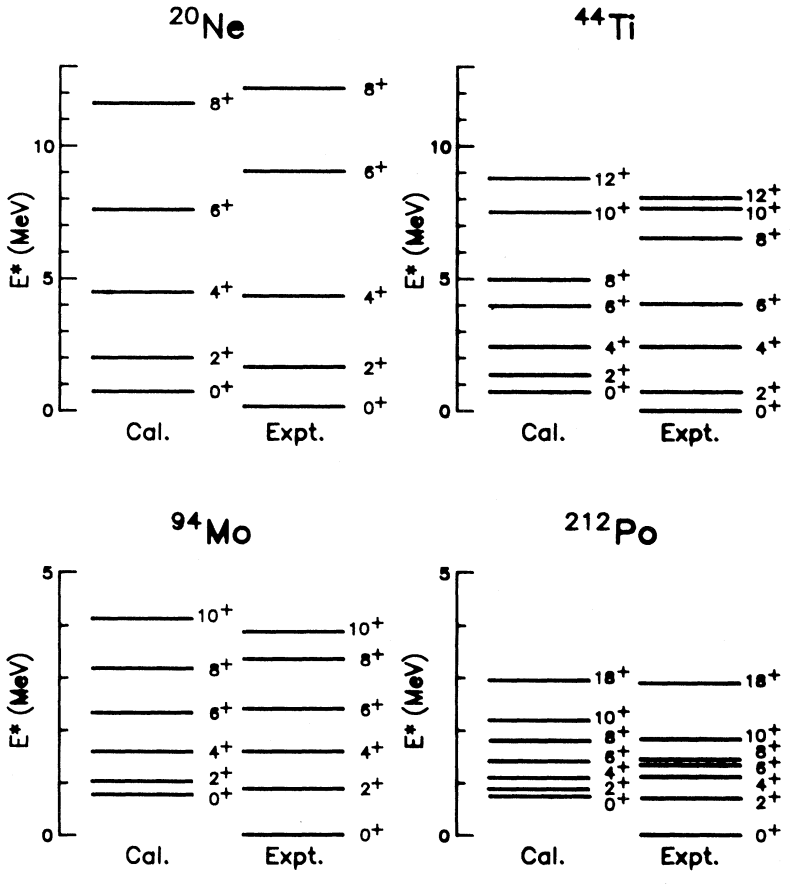

FIG. 2. Comparison of the calculated and measured α-core spectra for ^{20}Ne ($G = 8$), ^{44}Ti ($G = 12$), ^{94}Mo ($G = 16$), and ^{212}Po ($G = 20$). We use $V_0 = 220$ MeV, $a = 0.65$ fm, and $\alpha = 0.30$. Values for the radii R are given in Tables II and IV.

III. THE CHOICE OF PARAMETERS

We choose the adjustable parameters of our model to reproduce satisfactorily the large set of α-decay half-lives for even-even nuclei as in Ref. [11], as well as the experimental excitation energies of the states of ^{20}Ne, ^{44}Ti, ^{94}Mo, and ^{212}Po shown in Fig. 2 (except for the 0^+ ground states which we omit since, in common with earlier calculations for ^{20}Ne and ^{44}Ti [7–10], we systematically underbind them by ~ 0.7 MeV).

For consistency with previous work we take the α-preformation factors to be 1. The values of G for the ground state bands of the α + doubly closed LS-shell nuclei ^{20}Ne and ^{44}Ti can be confidently chosen as $G = 8$ and $G = 12$, respectively, and $G = 16$ for ^{94}Mo seems likely. For ^{212}Po the value $G = 22$ suggested by the simple shell model can be taken only as a rough guide since oscillator wave functions would not describe nuclear orbits at all well at high mass numbers. The information now available is that the presence of an 18^+ level in the ground state band of ^{212}Po requires $G(A > 208) \geq 18$, and that the alpha-decay half-lives of heavy nuclei are best fitted with $G(A > 208)$ in the range 18–24 [11]. We have investigated the various choices in some detail, and find that the best overall fit is obtained with the parameters deduced by using $G(A > 208) = 20$, but that the best description of ^{212}Po alone is obtained with $G(A > 208) = 18$.

We have then compared fits using diffuseness values of $a = 0.60$, 0.65, 0.70, and 0.75 fm. With the radii fitted to the α-separation energy, V_0 and α are chosen to minimize mean squared deviations S_E and $S_{\rm HL}$ of the calculated and measured excitation energies and logarithms of half-lives

$$S_E = \sum [E^{\rm expt}({\rm MeV}) - E^{\rm cal}({\rm MeV})]^2$$

and (6)

$$S_{\rm HL} = \sum [\log_{10} T^{\rm expt}_{1/2}({\rm s}) - \log_{10} T^{\rm cal}_{1/2}({\rm s})]^2 .$$

With $G(A > 208) = 20$, the four parameter sets shown in Table I all give an acceptable reproduction of the experimental quantities, with $a = 0.65$ or 0.70 fm providing the best results. Our preference for the former is based on the similarity of the shapes of the resulting α + ^{16}O and α + ^{40}Ca potentials to the real parts of the optical potentials deduced from elastic α scattering for these systems. The two potentials obtained for these systems from this prescription are compared with the extracted scattering potentials (with depth multiplied by 0.9 so as to reproduce the α-emission breakup threshold [7]) in Fig. 3. With this additional restriction we choose the set

$$\text{Potential 1}: \quad a = 0.65 \text{ fm}, \quad V_0 = 220 \text{ MeV}, \quad \alpha = 0.30, \tag{7}$$

for further global investigation. However, as discussed above, the choice

$$\text{Potential 2}: \quad a = 0.70 \text{ fm}, \quad V_0 = 200 \text{ MeV}, \quad \alpha = 0.30 \tag{8}$$

obtained from an overall fit with $G(A > 208) = 18$ would be preferable for a description of ^{212}Po.

TABLE I. Potential parameter values. Values of V_0, a and α which allow simultaneous good reproductions of α-decay half-lives in heavy nuclei and of spectra in ^{20}Ne ($G = 8$), ^{44}Ti ($G = 12$), ^{94}Mo ($G = 16$), and ^{212}Po ($G = 20$). See Eq. (6) and accompanying text for definitions of S_E and $S_{\rm HL}$.

a (fm)	V_0 (MeV)	α	S_E	$S_{\rm HL}$
0.60	215	0.25	5.113	3.353
0.65	220	0.30	4.401	2.588
0.70	230	0.35	3.989	2.913
0.75	235	0.40	5.418	3.134

IV. RESULTS

Figure 2 compares the semiclassically calculated energies of the ground state bands of α-cluster states in ^{20}Ne, ^{44}Ti, ^{94}Mo, and ^{212}Po with their experimental counterparts. Only the radius parameter R has been explicitly fitted to each nucleus, whereas V_0, a, and α remain the

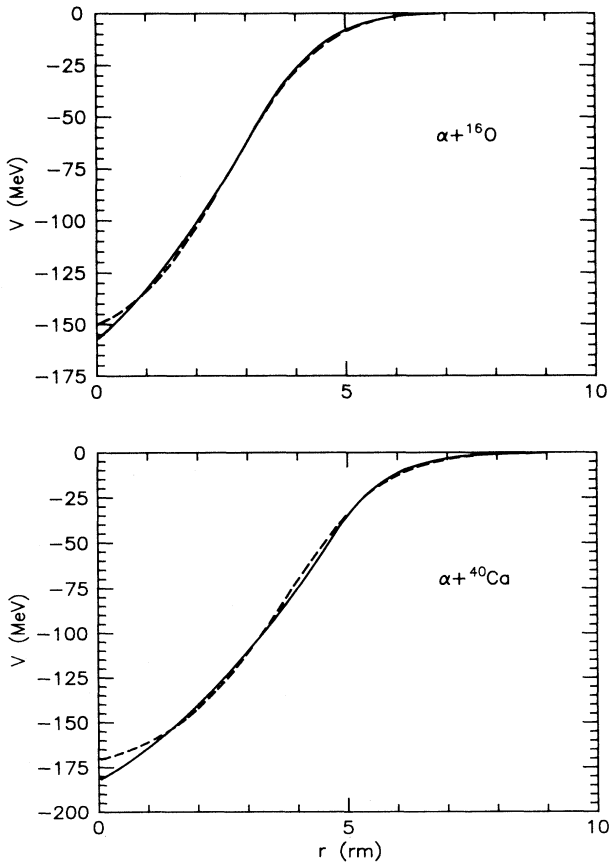

FIG. 3. Comparison of calculated (full lines) and optical (dashed lines) potentials for α + ^{16}O and α + ^{40}Ca.

same for all four. Nevertheless, the level of agreement between theory and experiment for each nucleus is at least as good, if not better, than that obtained by cluster models specifically targeted on a single nucleus. Remarkably, the trend of the spectra away from quasirotational spacings as the mass number increases from 20 to 212 has been achieved with a single geometric form for the nuclear potential.

This feature of compression of the higher levels of a band is actually already perceptible in ^{20}Ne, where the 8^+ state lies about 2 MeV below the position expected from pure rotational spacing. It is clearly manifest in ^{44}Ti, and is expected in ^{94}Mo and ^{212}Po although several predicted states have not yet been detected in these latter nuclei. In particular it provides an explanation of the isomerism of the 18^+ state in ^{212}Po. In this nucleus the upper band compression is so great that the final states are essentially degenerate (the 18^+ may even lie below the 16^+) so that the electromagnetic transition from the 18^+ is so slow that it cannot compete with a direct α decay to the ground state of ^{208}Pb.

The only blemish on our description of the spectra is that we systematically place the 0^+ bandhead about 0.7 MeV too close to the 2^+ in all cases. This may be due to an inadequate description of the shape of the potential near the origin where s states have finite amplitude. In our fits to spectra, we therefore choose the radii to reproduce the experimental energy of the 4^+ member rather than the 0^+ of each band.

Bands of negative parity states should also occur in these four nuclei. This expectation is well confirmed in ^{20}Ne, although there is some controversy about the correct identification of the 7^- and 9^- band members [17,18], while in ^{44}Ti the first three members of the negative parity band have only recently been discovered [5,6]. Further experimental work is necessary to search for the equivalent negative parity bands in ^{94}Mo and ^{212}Po.

Table II compares our calculated $B(E2\downarrow)$ reduced transition strengths with measured values for ^{20}Ne, ^{44}Ti, and ^{94}Mo. We evaluate these quantities with the wave functions $|G,L\rangle$ obtained from the single-particle Schrödinger equation (using the appropriate potential) and without introducing any effective charges. We have [19]

$$B(E2;\ G,L \rightarrow L-2) = \frac{15}{8\pi}\beta_2^2 \frac{L(L-1)}{(2L+1)(2L-1)} \langle r^2_{L,L-2}\rangle^2 \quad (9)$$

for a transition from L to $L-2$ involving spinless clusters and cores where the recoil factor is

$$\beta_2 = \frac{Z_1A_2^2 + Z_2A_1^2}{(A_1+A_2)^2} \quad (10)$$

with (Z_1, A_1) and (Z_2, A_2) the (charge, mass) numbers of the cluster and core.

The level of agreement between the theoretical calculations and the experimental data is generally very good. However, there is a tendency for the theory to underestimate the transition strengths as the mass number increases. This is probably because the calculated wave functions have too much strength in the nuclear interior, and ought to be more strongly peaked at the surface. This defect is less noticeable in the lightest nuclei since there the wave functions have very few nodes and are strongly peaked at the surface in any case, but it becomes more important as the number of nodes associated with low spin states increases with increasing mass number.

There is only a limited opportunity to test the predictions of our model against measured α-emission widths in ^{20}Ne, ^{44}Ti, and ^{94}Mo. Most of the positive parity α-cluster band members in these nuclei are either bound against α emission, or else their widths have not been experimentally determined. However, if we examine the excited negative parity α-cluster band states as well, it is possible to make a limited test of our model predictions in ^{20}Ne. Table III compares our results for α_0-decay widths with measured values and with the earlier calculations of Buck, Dover, and Vary [3]. We have calculated these widths by slightly adjusting the potential radius to yield a quasistationary state with $2n + L = 8, 9$ at the experimentally known excitation energy of each individual state, and then solving the single-particle Schrödinger equation with complex arithmetic with Gamow tails fitted to the wave functions (using the code GAMOW [20]). Our results are inferior to those of Ref. [3], although still acceptable, and suggest that a fine-tuning of the parame-

TABLE II. $B(E2\downarrow)$ values. Calculated and measured $B(E2\downarrow)$ values (in e^2 fm^4) for ^{20}Ne, ^{44}Ti, and ^{94}Mo.

Nucleus	Transition	$B(E2\downarrow)_{\rm calc}$	$B(E2\downarrow)_{\rm expt}$
^{20}Ne	$2^+(1.63\ \text{MeV}) \rightarrow 0^+(0.00\ \text{MeV})$	47	68 ± 4
(R=3.284 fm)	$4^+(4.25\ \text{MeV}) \rightarrow 2^+(1.63\ \text{MeV})$	60	71 ± 7
	$6^+(8.78\ \text{MeV}) \rightarrow 4^+(4.25\ \text{MeV})$	48	65 ± 10
	$8^+(11.95\ \text{MeV}) \rightarrow 6^+(8.78\ \text{MeV})$	24	30 ± 4
^{44}Ti	$2^+(0.72\ \text{MeV}) \rightarrow 0^+(0.00\ \text{MeV})$	102	120 ± 37
(R=4.560 fm)	$4^+(2.45\ \text{MeV}) \rightarrow 2^+(0.72\ \text{MeV})$	136	277 ± 55
	$6^+(4.02\ \text{MeV}) \rightarrow 4^+(2.45\ \text{MeV})$	130	157 ± 28
	$8^+(6.51\ \text{MeV}) \rightarrow 6^+(4.02\ \text{MeV})$	106	> 14
	$10^+(7.67\ \text{MeV}) \rightarrow 8^+(6.51\ \text{MeV})$	72	138 ± 28
	$12^+(8.04\ \text{MeV}) \rightarrow 10^+(7.67\ \text{MeV})$	35	< 60
^{94}Mo	$2^+(0.87\ \text{MeV}) \rightarrow 0^+(0.00\ \text{MeV})$	199	391 ± 5
(R=5.793 fm)	$4^+(1.57\ \text{MeV}) \rightarrow 2^+(0.87\ \text{MeV})$	272	660 ± 101

TABLE III. α_0 widths in ^{20}Ne. Calculated and measured α_0-emission widths of α-cluster states in ^{20}Ne.

J^π	Excitation energy (MeV)	Γ_{α_0} (keV) (experiment)	Γ_{α_0} (keV) (potential 1)	Γ_{α_0} (keV) (Ref. [3])
6^+	8.776	0.11 ± 0.02	0.57	0.21
8^+	11.951	0.035 ± 0.010	0.35	0.108
1^-	5.7877	0.028 ± 0.003	0.038	0.021
3^-	7.1563	8.2 ± 0.3	11.0	6.7
5^-	10.262	145 ± 40	172	81
7^-	13.692	158 ± 15	117	—
{7^-	15.336	78 ± 7	485	183}
9^-	17.430	53 ± 6	15.0	—
{9^-	22.87	$< 225 \pm 40$	546	—}

ter values of the global potential is necessary to reproduce the detailed features of a given nucleus. We also note that the identification of the best experimental candidates for the 7^- and 9^- members of the α-cluster band has been changed from states at 15.336 MeV and 22.87 MeV, respectively [17], to states at 13.692 MeV and 17.430 MeV, respectively [18]. We include calculations for both pairs of states in Table III, and a comparison of our calculated α_0 widths with the experimental values favors the new assignments [18].

In ^{212}Po, α decay to the ground state of ^{208}Pb offers significant competition to $E2$ γ decay. It is therefore more illuminating to evaluate α- and γ-decay widths Γ_α and Γ_γ and then to compute half-lives and α-branching ratios for comparison with experiment. To evaluate Γ_γ we use the same potential as for the ^{212}Po spectrum, and relate the width to the $B(E2\downarrow)$ values by

$$\Gamma_\gamma(\mathrm{MeV}) = 8.070 \times 10^{-13} E_\gamma^5 (1+\alpha_T) \times B(E2;\ L_i \to L_f, e^2\ \mathrm{fm}^4), \quad (11)$$

where E_γ is the γ-ray energy in MeV, and α_T is the appropriate internal conversion coefficient. However, for the α decays it is essential to have the calculated state at the exact experimental energy so as to evaluate the correct barrier penetration factor, and so R is individually tailored to each state to ensure this. The smallness of the variations in R (see Table IV) is a measure of the adequacy of our assumed geometric form for the α-^{208}Pb potential.

Table IV lists the excitation energies [21] of the known members of the ground state band of ^{212}Po together with the calculated values of R, Γ_α, and Γ_γ for both potential 1 and potential 2. The Q value for α decay from a state (G, L) in ^{212}Po to the ground state of ^{208}Pb is given by

$$Q(G,L) = Q(G,0) + E^*(G,L), \quad (12)$$

where $Q(G,0) = 8.986$ MeV includes a small electron shielding correction [11] and $E^*(G,L)$ is the excitation energy of the state in ^{212}Po. This, together with the internal conversion coefficients α_T and the parameter values of Eq. (7), is sufficient to obtain values for R, Γ_α, and Γ_γ within our model. In terms of the widths Γ_α and Γ_γ, the half-life $T_{1/2}$ and α-branching ratio b_α are given by

$$T_{1/2} = \frac{\hbar \ln 2}{\Gamma_\alpha + \Gamma_\gamma}, \quad b_\alpha = \frac{\Gamma_\alpha}{\Gamma_\alpha + \Gamma_\gamma}, \quad (13)$$

where $\hbar = 6.582 \times 10^{-22}$ MeV s. Using the values of the widths from Table IV, we calculate $T_{1/2}$ and b_α, and in Table V compare our results with the corresponding experimental values. For the half-lives $T_{1/2}$ the agreement is generally good and this enables us to make confident predictions of $T_{1/2}$ for the 2^+ and 4^+ members of the band. Only the 18^+ half-life prediction lies more than a factor ~ 3 from the corresponding measurement, and we see that potential 2 gives a significantly better result than potential 1 for this value. Although we reproduce the general trend, the agreement for the branching ratios is substantially poorer (to within a factor ~ 5). We note, however, that the branching ratios are either very small, or imperfectly known [21], and further experimental work may well reduce these discrepancies. We note further that our predictions for the lifetimes are independent of the observed values of these branching ratios.

V. CONCLUSIONS

We have given a good account of the evolving patterns of excitation energies of the members of the ground state band of ^{20}Ne, ^{44}Ti, ^{94}Mo, and ^{212}Po using an α-cluster model which employs a potential with fixed depth V_0, diffuseness a and mixing parameter α. Only the radius R is specifically tailored to the given nucleus. We go

TABLE IV. α and γ widths in ^{212}Po: α and γ widths in ^{212}Po calculated using the two potentials of Eqs. (7) and (8).

J^π	E^* (MeV)	α_T	R (fm) (pot. 1, pot. 2)	Γ_α (MeV) (pot. 1, pot. 2)	Γ_γ (MeV) (pot. 1, pot. 2)
0^+	0.000	—	(7.051, 6.989)	$(4.43, 3.56) \times 10^{-15}$	0
2^+	0.727	0.014	(7.030, 6.967)	$(10.6, 8.53) \times 10^{-14}$	$(6.25, 5.90) \times 10^{-11}$
4^+	1.133	0.055	(7.025, 6.963)	$(1.94, 1.54) \times 10^{-13}$	$(4.88, 4.59) \times 10^{-12}$
6^+	1.356	0.329	(7.029, 6.970)	$(7.11, 5.46) \times 10^{-14}$	$(3.18, 2.97) \times 10^{-13}$
8^+	1.476	3.310	(7.036, 6.981)	$(8.18, 5.99) \times 10^{-15}$	$(4.43, 4.09) \times 10^{-14}$
10^+	1.834	0.077	(7.037, 6.984)	$(1.33, 0.91) \times 10^{-15}$	$(2.37, 2.14) \times 10^{-12}$
(18^+)	2.922	$\gg 1$	(7.027, 6.978)	$(2.48, 0.52) \times 10^{-22}$	0[a]

[a]Not calculated. Multipolarity of primary transition uncertain, with $\Gamma_\gamma \ll \Gamma_\alpha$ [18].

TABLE V. $T_{1/2}$ and b_α values in ^{212}Po: A comparison of the half-lives and α-branching ratios for the members of the ground state band of ^{212}Po, calculated using the two potentials of Eqs. (7) and (8), with experimental data.

J^π	E^* (MeV)	$T_{\frac{1}{2}}$ (expt)	$T_{\frac{1}{2}}$ (calc) (pot. 1, pot. 2)	b_α % (expt)	b_α % (calc) (pot. 1, pot. 2)
0^+	0.000	0.30 μs	(0.10, 0.13) μs	100	100
2^+	0.727	—	(7.3, 7.7) ps	0.033	(0.17, 0.14)
4^+	1.133	—	(90, 96) ps	~ 27	(3.8, 3.2)
6^+	1.356	(0.76 ± 0.21) ns	(1.2, 1.3) ns	~ 71	(18, 16)
8^+	1.476	17 ns	(8.7, 9.7) ns	~ 42 (or 6 ± 1)	(16, 13)
10^+	1.834	(0.55 ± 0.14) ns	(0.19, 0.21) ns	no α particle detected	(0.06, 0.04)
(18^+)	2.922	45 s	(1.8, 8.7) s	99.93	100

a long way towards reproducing the strongly enhanced $E2$ transition strengths within these bands without introducing effective charges. Our potential form also accounts for the α-decay half-lives of many heavy nuclei, and closely approximates the real part of the optical potential for α-^{16}O and α-^{40}Ca. Our results stand comparison with cluster model treatments of individual nuclei, and in ^{212}Po are superior to limited basis shell model calculations [14,22] for the states under consideration. The most important conclusion to be drawn is that there is considerable α clustering in heavy nuclei and that simple models can elucidate their spectroscopic features. In particular, there appears to be a significant degree of such clustering in ^{212}Po.

A.C.M. would like to thank the U.K. Engineering and Physical Sciences Research Council for financial support.

[1] K. Wildermuth and Y.C. Tang, *A Unified Theory of the Nucleus* (Academic Press, New York, 1977), p. 1.
[2] H. Furutani, H. Kanada, T. Kaneko, S. Nagata, H. Nishioka, S. Okabe, S. Saito, T. Sakuda, and M. Seya, Prog. Theor. Phys. Suppl. **68**, 193 (1980).
[3] B. Buck, C.B. Dover, and J.P. Vary, Phys. Rev. C **11**, 1803 (1975).
[4] K.F. Pal and R.G. Lovas, Phys. Lett. **96B**, 19 (1980).
[5] T. Yamaya, S. Oh-Ami, M. Fujiwara, T. Itahashi, K. Katori, M. Tosaki, S. Kato, S. Hatori, and S. Ohkubo, Phys. Rev. C **42**, 1935 (1990).
[6] P. Guazzoni, M. Jaskola, L. Zetta, C.-Y. Kim, T. Udagawa, and G. Bohlen, Nucl. Phys. **A564**, 425 (1993).
[7] F. Michel, G. Reidemeister, and S. Ohkubo, Phys. Rev. Lett. **57**, 1215 (1986); Phys. Rev. C **37**, 292 (1988).
[8] T. Wada and H. Horiuchi, Phys. Rev. Lett. **58**, 2190 (1987); Phys. Rev. C **38**, 2063 (1988).
[9] A.C. Merchant, K.F. Pal, and P.E. Hodgson, J. Phys. G **15**, 601 (1989).
[10] Th. Delbar, C. Grégoire, G. Paic, R. Ceulneer, F. Michel, R. Vanderpoorten, A. Budzanowski, H. Dabrowski, L. Freindl, K. Grotowski, S. Micek, R. Planeta, A. Strzalkowski, and K. Eberhard, Phys. Rev. C **18**, 1237 (1978).
[11] B. Buck, A.C. Merchant, and S.M. Perez, Phys. Rev. Lett. **65**, 2975 (1990); Phys. Rev. C **45**, 2247 (1992).
[12] B. Buck, A.C. Merchant, and S.M. Perez, At. Data Nucl. Data Tables **54**, 53 (1993).
[13] K. Varga, R.G. Lovas, and R.J. Liotta, Phys. Rev. Lett. **69**, 37 (1992); Nucl. Phys. **A550**, 421 (1992).
[14] B. Buck, A.C. Merchant, and S.M. Perez, Phys. Rev. Lett. **72**, 1326 (1994).
[15] F. Michel, J. Albinski, P. Belery, Th. Delbar, C. Grégoire, B. Tasiaux, and G. Reidemeister, Phys. Rev. C **28**, 1904 (1983).
[16] S.A. Gurvitz and G. Kälbermann, Phys. Rev. Lett. **59**, 262 (1987).
[17] F. Ajzenberg-Selove, Nucl. Phys. **A392**, 1 (1983).
[18] F. Ajzenberg-Selove, Nucl. Phys. **A475**, 1 (1987).
[19] B. Buck and A.A. Pilt, Nucl. Phys. **A280**, 133 (1977).
[20] T. Vertse, K.F. Pal, and Z. Balogh, Comput. Phys. Commun. **27**, 309 (1982).
[21] A. Arta-Cohen, Nucl. Data Sheets **66**, 171 (1992).
[22] A.R. Poletti, G.D. Dracoulis, A.P. Byrne, and A.E. Stuchbery, Nucl. Phys. **A473**, 595 (1987).